

Effect of power output on muscle coordination during rowing

Nicolas A. Turpin · Arnaud Guével · Sylvain Durand · François Hug

Received: 23 November 2010 / Accepted: 15 March 2011
© Springer-Verlag 2011

Abstract The present study was designed to quantify the effect of power output on muscle coordination during rowing. Surface electromyographic (EMG) activity of 23 muscles and mechanical variables were recorded in eight untrained subjects and seven experienced rowers. Each subject was asked to perform three 2-min constant-load exercises performed at 60, 90 and 120% of the mean power output over a maximal 2,000-m event (denoted as P60, P90, and P120, respectively). A decomposition algorithm (nonnegative matrix factorization) was used to extract the muscle synergies that represent the global temporal and spatial organization of the motor output. The results showed a main effect of power output for 22 of 23 muscles (p values ranged from <0.0001 to 0.004) indicating a significant increase in EMG activity level with power output for both untrained and experienced subjects. However, for the two populations, no dramatic modification in the shape of individual EMG patterns (mean r_{\max} value = 0.93 ± 0.09) or in their timing of activation (maximum lag time = $-4.3 \pm 3.8\%$ of the rowing cycle) was found. The results also showed a large consistency of the three extracted muscle synergies, for both synergy activation coefficients (mean r_{\max} values range from 0.87 to 0.97) and muscle synergy vectors (mean r values range from 0.70 to

0.76) across the three power outputs. In conclusion, despite significant changes in the level of muscle activity, the global temporal and spatial organization of the motor output is very little affected by power output on a rowing ergometer.

Keywords Electromyography · Muscle synergy · Rowers · Workload · Modules

Introduction

Rowing is an Olympic discipline that requires performing 2,000 m as fast as possible at a mean power output of 300–450 W for trained rowers (Soper and Hume 2004). While the physiological and biomechanical parameters associated with rowing performance have been largely studied (Hagerman 1984; Soper and Hume 2004; Volianitis and Secher 2009), few data are available about muscle coordination [defined as “a distribution of muscle activation or force among individual muscles to produce a given combination of joint moments” (Prilutsky 2000)]. Using surface electromyography (EMG), some studies have reported muscle activity patterns on a rowing ergometer (Lay et al. 2002; Pollock et al. 2009; Rodriguez et al. 1990; Wilson et al. 1988). However, despite that rowing involves numerous muscles and requires the skilled coordination of the upper and lower limbs (Rodriguez et al. 1990; Soper and Hume 2004) these studies recorded a limited number of muscles (up to 12 muscles). Additionally, no studies have explored the putative changes in muscle coordination in response to changes in power output, as already reported in other tasks such as pedaling (Jorge and Hull 1986; Wakeling et al. 2010) and running (Slawinski et al. 2008). Because kinematics and force profiles change with rowing

Communicated by Susan A. Ward.

N. A. Turpin · A. Guével · F. Hug (✉)
Laboratory «Motricité, Interactions, Performance» (EA 4334),
University of Nantes, 25 bis boulevard Guy Mollet,
BP 72206, 44322 Nantes cedex 3, France
e-mail: francois.hug@univ-nantes.fr

S. Durand
Laboratory «Motricité, Interactions, Performance» (EA 4334),
University of Maine, 72000 Le Mans, France

intensity (McGregor et al. 2004, 2005), it would be expected that muscle coordination is also modified. It is critical to address this question because training usually includes rowing sessions at different power outputs, generally at lower power outputs than generated during a competition. Thus, muscle coordination is not necessarily the same during training and competition.

Studies focusing on muscle coordination usually report muscle activity profiles of individual muscles, i.e., EMG patterns. From this EMG profile, information about muscle activation timing, shape of muscle activity and muscle activity level can be extracted (for review, see Hug 2011). Recently, a technique has emerged that is capable of decomposing EMG patterns recorded from numerous muscles into the summed activation of just a few muscle synergies (Ting and McKay 2007; Tresch et al. 1999). Muscle synergies represent the global temporal and spatial organization of the motor output (Li 2006) and provide an attractive simplified strategy for the control of complex movements because they reduce the number of output patterns that the nervous system must specify for a large number of muscles (Raasch and Zajac 1999). For example, five muscle synergies account for the majority of variability in the surface EMG signals of 32 muscles during walking (Ivanenko et al. 2006) and running (Cappellini et al. 2006). Recently, it has been reported that pedaling in a population of trained cyclists is accomplished by the combination of three muscle synergies (Hug et al. 2010). In combination with a traditional EMG analysis, extraction of muscle synergy is useful to study whether changes in individual EMG pattern would induce changes in the muscle synergies and thus in the motor control strategies (Hug 2011; Ting and Chvatal 2010).

The present study was designed to quantify the effect of power output on muscle coordination during rowing in both untrained subjects and experienced rowers. Surface EMG activity was recorded in 23 muscles during three rowing exercises performed at different power outputs on a rowing ergometer. To better describe the muscle coordination strategies, a non-negative matrix factorization algorithm was used to identify the muscle synergies in addition to a classical analysis of individual EMG patterns. We hypothesized that the temporal and spatial organization of the motor output would be modified by power output, inducing the changes in mechanical patterns reported in the literature.

Materials and methods

Subjects

Eight male untrained subjects (UNT, age 24 ± 5 years, height 179 ± 9 cm, body mass 70 ± 6 kg), and seven

male experienced national-level rowers (EXP, age 25 ± 3 years, height 187 ± 4 cm, body mass 81 ± 11 kg) volunteered to participate in this study. UNT practiced recreational activities but had no prior experience with rowing (neither on ergometer nor on water). EXP had 10.4 ± 4.2 years of competitive olympic rowing experience and trained for approximately 11.6 ± 3.2 h per week at the time of the study. They had performed an all-out 2,000 m rowing test in 390 ± 15 s in the same year of this experiment. All subjects were informed of the possible risk and discomfort associated with the experimental procedures prior to giving their written consent to participate. The experimental design of the study was approved by the local Ethical Committee and was conducted in accordance with the Declaration of Helsinki.

Procedure

The tests were divided into two identical sessions to allow for the measurement of 23 muscles. One week before the first session, UNT performed an all-out 2,000 m rowing test on an ergometer (Rowperfect, Harbord, Australia) to assess their mean power (MP) over this distance. This test consisted in a standardized warm up of 5 min at a low-perceived effort, followed by 2 min of recovery. Subjects were then asked to perform 2,000-m as fast as possible. For EXP, the MP was taken from training data (i.e., time to perform a 2,000-m rowing) before the official experiments. The estimate of MP in watts was determined according to the following equation:

$$MP = 2.8 \left(\frac{2,000}{t_{2,000}} \right)^3 \quad (1)$$

where $t_{2,000}$ is the time to perform the 2,000 m (in s). This formula is based on the power required to keep a boat moving at a constant velocity, and 2.8 is a typical drag coefficient for a racing shell (Gordon 2003).

Subjects were first asked to perform a standardized warm-up consisting of 5 min of rowing at a self-paced intensity followed by three 2-min constant-load exercises performed at 60, 90 and 120% of MP (denoted as P60, P90, and P120, respectively). A 2-min recovery period was placed between each bout. These intensities were chosen based on the knowledge of the pacing strategies of a 2,000-m race (Soper and Hume 2004). In fact, while 120% of MP corresponds to the highest intensity adopted during a 2,000-m race (during the first 500-m), 90% of MP corresponds to the lowest intensity observed during this event (Soper and Hume 2004). Sixty percent of MP corresponds to a classical training intensity. In order to reduce the chance of fatigue influencing EMG patterns only the first minute of P120 was analyzed.

Materials and data collection

Subjects exercised on a rowing ergometer (Rowperfect, Harbord, Australia) with a fixed stretcher mechanism (Fig. 1). As described previously (Colloud et al. 2006), the ergometer was instrumented to measure the force produced at the handle with a strain gauge force transducer (SM-1000N; Interface™, Scottsdale, AZ, USA), which was placed in series with the chain and the handle using a ball-and-socket joint (free to rotate in three degrees of freedom). Additionally, a position sensor (PT1 Scaime™, Annemasse, France) was installed on the chain. The right stretcher was equipped with four home-built bi-directional (antero-posterior and vertical axes) strain-gauge transducers (measurement range 1,500 N, tolerance of overload 750 N, linearity 0.15%, hysteresis 0.02%) to record the stretcher force of the subjects (Colloud et al. 2006). The stretcher formed a 45° angle with horizontal. The antero-posterior and vertical stretcher forces were calculated using the data provided by the stretcher transducers. All mechanical signals were sampled at 125 Hz with an acquisition device (DT 9804, Data Translation™, Malboro, MA, USA) and digitally stored using acquisition software (Data-Foundry version 5.1, Data Translation). A visual feedback of the power output and stroke frequency was displayed on a monitor placed in front of the subjects throughout the experimental protocol. The power displayed to the participants represents the average power over an entire cycle as depicted by Boyas et al. (2006).

Surface EMG was recorded from 23 muscles on the right side of the body in two separate sessions interspaced by 4 days–1 week. The recorded muscles in the first session were tibialis Anterior (TA), soleus (Sol), gastrocnemius lateralis (GL), gastrocnemius medialis (GM), vastus lateralis (VL), vastus medialis (VM), rectus femoris (RF), biceps femoris (BF), semitendinosus (ST), gluteus maximus (GMax), latissimus dorsi (LD), erector spinae multifidus (ES), trapezius medius (TraM), biceps brachii (BB) and brachioradialis (Br). In the second session, the

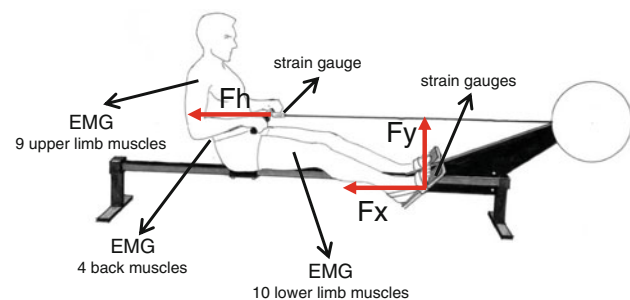


Fig. 1 Experimental design. Subjects exercised on a rowing ergometer with a fixed stretcher mechanism that was instrumented to measure the forces produced at the handle (F_h) and at the right stretcher (F_x and F_y). Surface EMG was recorded from 23 muscles on the right side of the body in two separate sessions

following muscles were recorded: longissimus (Long), iliocostallis (Ilio), multifidus (ES), latissimus dorsi (LD), deltoideus posterior (Delt), trapezius upper (TraU), trapezius medius (TraM), trapezius lower (TraL), triceps brachii (long head—TriL), triceps brachii (short head—TriS), biceps brachii (BB), brachioradialis (Br) and flexor digitorum superficialis (FD). Five out of the 23 muscles were recorded during both of the two sessions in order to check the consistency of muscle coordination between the two sessions. For these muscles, only the first session was taken into consideration for further analysis. For each muscle, a dry-surface electrode (Delsys DE 2.1, Delsys Inc, Boston, MA, USA; 1 cm interelectrode distance) was attached to the skin. Prior to electrode application, the skin was shaved and cleaned with a mixture of alcohol and ether to minimize impedance. Each electrode was placed longitudinally with respect to the underlying muscle fiber arrangement and all were located according to the recommendations of Surface EMG for Non-Invasive Assessment of Muscles (SENIAM) (Hermens et al. 2000) for all of the muscles, except for the muscles latissimus dorsi (LD), brachioradialis (Br), and flexor digitorum (FD) which are not referenced by SENIAM. For LD, the electrode was placed as recommended by de Sèze and Cazalets (2008), i.e., over the muscular curve at T12 and along a line connecting the most posterior point of the posterior axillary fold and the S2 spinous process. For Br, the electrode was positioned as done by Muceli et al. (2010), i.e., 1/6 of the distance from the midpoint between the cubit fossa to the lateral epicondyle to the styloid process of the ulna. For FD, the electrode was positioned at 1/5 of the distance from the medial humeral epicondyle to the styloid process of the ulna (Zipp 1982). The wires connected to the electrodes were well secured with adhesive tape to avoid movement-induced artifacts. EMG signals were amplified ($\times 1,000$) and digitized (6–400 Hz bandwidth) at a sampling rate of 1 kHz (Bagnoli 16, Delsys), and stored on a computer.

Data processing

Electromyographic signals were filtered with a bandpass filter (4th order Butterworth) between 20 and 400 Hz (filtfilt function of Matlab, the Mathworks, version R2007b, Natick, MA, USA). A band-stop filter (48–52 Hz) was used to remove the 50-Hz noise. Linear envelopes for each muscle were obtained by low-pass filtering the fully rectified EMG signals with an 8-Hz low-pass filter (zero lag) as recommended by Shiavi et al. (1998). Each rowing cycle (period between two successive catches) was interpolated to 200 time points. A set of 15 consecutive cycles was extracted from a period of constant power output (i.e., the period between 0 and 20 s was not considered) and averaged to obtain a representative pattern for each muscle.

Then, as previously described (Hug et al. 2010), a non-negative matrix factorization was performed to extract muscle synergies. For this purpose, we implemented the Lee and Seung (2001) algorithm. Matrix factorization minimizes the residual Frobenius norm between the initial matrix and its decomposition, given as

$$\mathbf{E} = \mathbf{WC} + \mathbf{e} \quad (2)$$

$$\min_{\substack{\mathbf{W} \geq 0 \\ \mathbf{C} \geq 0}} \|\mathbf{E} - \mathbf{WC}\|_{FRO}$$

where \mathbf{E} is a p -by- n initial matrix (p = number of muscles and n = number of time points), \mathbf{W} is a p -by- s matrix (s = number of synergies), \mathbf{C} is an s -by- n matrix and \mathbf{e} is a p -by- n matrix. $\|\cdot\|_{FRO}$ establishes the Frobenius norm, \mathbf{W} represents the muscle synergy vectors matrix, \mathbf{C} is the synergy activation coefficients matrix and \mathbf{e} is the residual error matrix. While the “muscle synergy vectors” represent the relative weighting of each muscle within each synergy, the “synergy activation coefficient” represents the relative activation of the muscle synergy across the rowing cycle (for more details, see Fig. 1 from Hug et al. 2010). The algorithm is based on iterative updates of an initial random guess of \mathbf{W} and \mathbf{C} that converge to a local optimal matrix factorization [see Lee and Seung (2001) for more details]. To avoid local minima, the algorithm was repeated ten times for each subject. The lowest cost solution was retained (i.e., minimizing the squared errors between original and reconstructed EMG patterns). The initial matrix \mathbf{E} consisted of a cycle for each of the 23 muscles (the two sessions were pooled). \mathbf{E} was thus a 23 row by 200 column matrix. Each line of \mathbf{E} and \mathbf{C} was normalized by its maximum value. At P120, for each subject, we iterated the analysis by varying the number of synergies between 1 and 23 and selected the least number of synergies that accounted for >90% of the variance accounted for (VAF) (Hug et al. 2010; Torres-Oviedo et al. 2006). For the two other power outputs (i.e., P60 and 90), we kept the number of muscle synergies extracted at P120 for each subject. According to Torres-Oviedo et al. (2006), VAF was defined as

$$VAF = 1 - \frac{\sum_{i=1}^p \sum_{j=1}^n (\mathbf{e}_{ij})^2}{\sum_{i=1}^p \sum_{j=1}^n (\mathbf{E}_{ij})^2} \quad (3)$$

where subscript i goes from 1 to p the number of muscles, and j goes from 1 to n the number of time points.

The rowing cycle corresponded to the period between two successive catches. The catches are identified by means of the minimum in the position curve of the handle and the transition time to the maximum of this curve (Colloud et al. 2006). The rowing cycle was divided into drive (or propulsive) and recovery phases. The drive phase

ranged from 0 to 100% and the recovery phase from -100 to 0%, as in previous studies (Janshen et al. 2009; Pollock et al. 2009). Drive and recovery phases were re-sampled 100 time-points each. This time-scale normalization was used for comparing EMG patterns, mechanical patterns and synergy activation coefficients, ensuring robust comparisons by avoiding a possible bias due to different transition times between subjects (i.e., different duration of the drive and recovery phases among subjects) (Hug 2011). Note that this normalization procedure was not applied prior to muscle synergy extraction.

Statistical analysis

Data distributions consistently passed the Shapiro–Wilk normality test (Statistica[®]V6, Statsoft, Maison-Alfort, France). Values are therefore reported as mean \pm SD. Pearson’s correlation coefficient (r) was used as a similarity criterion for the muscle synergy vectors. Modification of the individual EMG patterns, mechanical patterns and synergy activation coefficients were assessed using two criteria: the lag time and r_{\max} coefficient. The lag times assess differences in the timing of the activations (i.e., the magnitude of the time shift between EMG patterns or between synergy activation coefficients) and were calculated as the lag time at the maximum of the cross-correlation function obtained using the Matlab x_{corr} function for centered data (option = “coeff”). r_{\max} corresponds to the correlation coefficient at this maximum of the cross-correlation function and gives an indication on the similarity of the waveforms (i.e., the shape of the EMG, mechanical and synergy activation coefficients). As performed in previous studies (Cappellini et al. 2006; Ivanenko et al. 2004), r_{\max} and r -statistics were based on Z-transformed values. A one-factor analysis of variance (ANOVA) (factor = expertise) with repeated measures (power output) was used to compare the similarities across populations (i.e., EXP vs. UNT) and across power-outputs. Post hoc analyses were performed using the Tukey’s method. One-sample Student’s t tests were performed to evaluate the differences in the lag time values from a reference value (i.e., zero). A p value below 0.05 was considered statistically significant.

Results

Mechanical data

For each of the three tests, EXP rowed at a significantly higher power output than UNT ($p < 0.05$). Power output at P60, P90 and P120 was 245.4 ± 40.7 , 346.9 ± 48.4 and 451.7 ± 54.0 W for EXP and 136.6 ± 19.9 , 195.5 ± 26.6 and 265.9 ± 35.1 W for UNT, respectively.

The stroke frequency analysis revealed a significant main effect of power output ($p < 0.001$) and expertise ($p = 0.008$). The main effects demonstrated that the stroke frequency increased as a function of power output (27.6 ± 2.3 , 29.0 ± 1.7 and 31.3 ± 1.2 strokes min^{-1} for P60, P90 and P120, respectively) and was significantly higher in UNT than EXP. More precisely, a post hoc analysis showed a significantly higher stroke frequency for UNT compared with EXP at P60.

Figure 2 depicts the ensemble average of the mechanical patterns for the two populations. The ANOVA showed a main effect of power output for the amplitude (lmax – minl) of all of these parameters (i.e., Fx, Fy and Fh), indicating a significant increase with power output for

both populations. The analysis also revealed the main effect of expertise on the amplitude only for Fx ($p < 0.001$) and Fh ($p < 0.001$). A significant interaction of power output \times expertise was observed for amplitude only for Fx ($p = 0.003$). More precisely, the increase in Fx amplitude was lower in UNT than EXP between P60 and P90 and between P90 and P120 (Fig. 2).

The r_{max} was computed as a similarity index of the shape of the mechanical patterns between power output conditions for both populations. Overall, very high r_{max} values (mean r_{max} across the three comparisons = 0.98 ± 0.02 , 0.98 ± 0.02 , 0.99 ± 0.01 , and 0.99 ± 0.01 for Fx, Fy, Fh, and power, respectively) were found indicating that the shapes of the mechanical patterns were not affected by power output.

Fig. 2 Ensemble averaged mechanical patterns for the two populations. The vertical dashed line indicates the transition between the recovery and drive phases (-100 to 0% represents the recovery phase and 0–100% represents the drive phase). Fx horizontal component of the right footstretcher force (N), Fy vertical component of the footstretcher force (N), Fh handle force (N), power instantaneous power (W), UNT untrained subjects, EXP experienced rowers. P60 is in black, P90 in light gray (or green) and P120 in dark gray (or red)

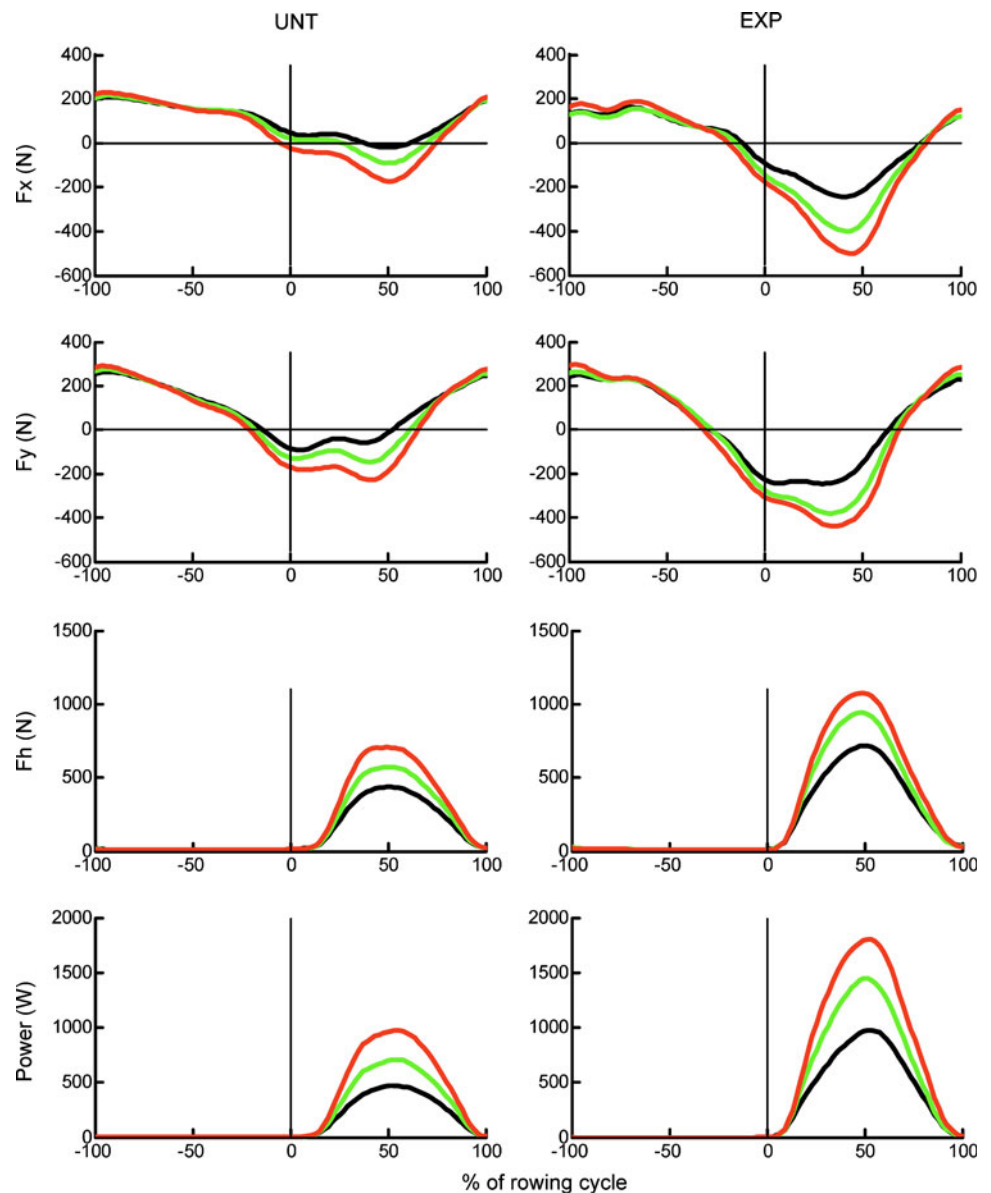
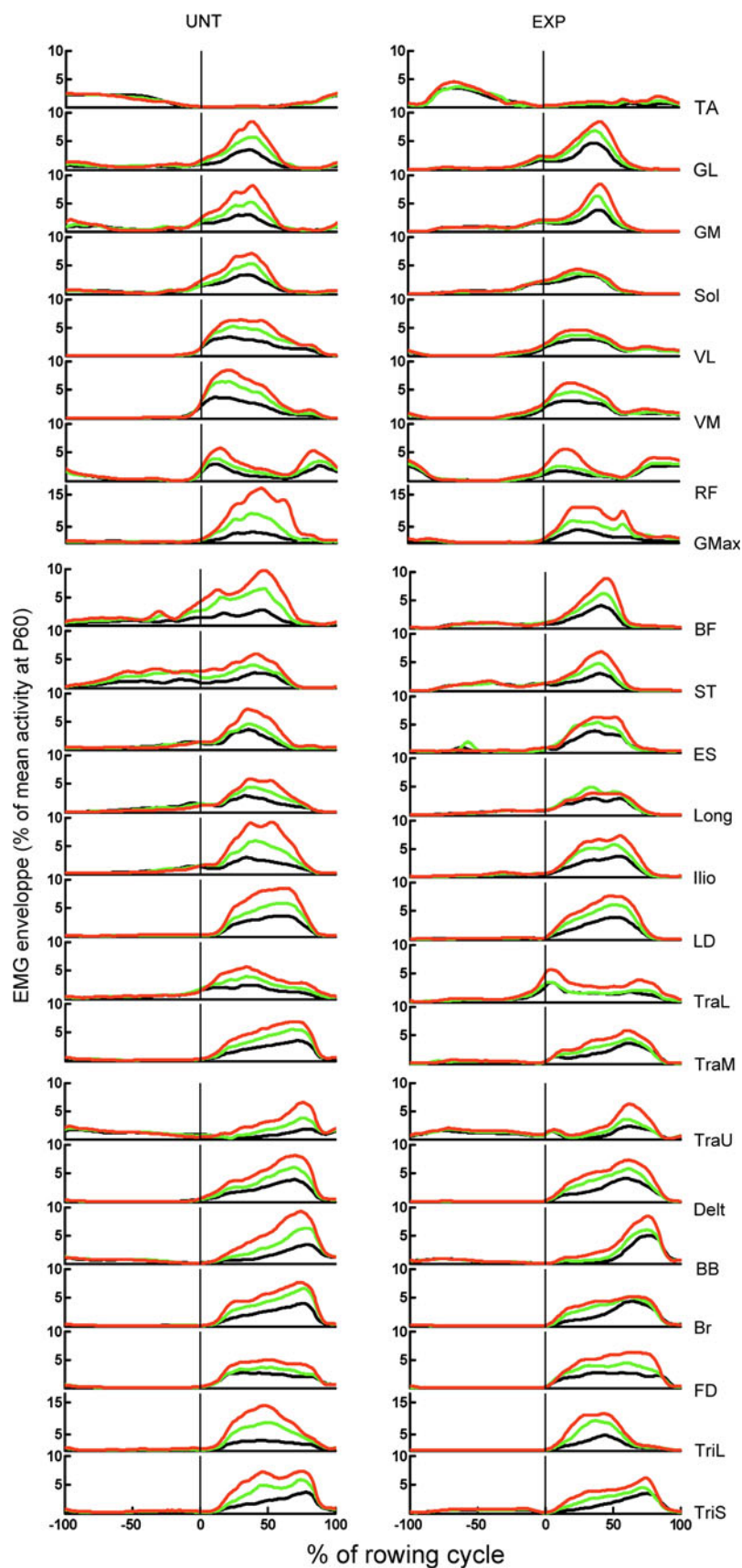


Fig. 3 Ensemble averaged EMG patterns of the 23 recorded muscles and for the two populations. The *vertical line* indicates the transition between the recovery and the drive phases (-100 to 0% represents the recovery phase and 0 – 100% represents the drive phase). EMG patterns for each subject are normalized by the averaged EMG at P60 and then averaged across subjects. For sake of clarity, the y axis for GMax and TriL was changed and is therefore different from the other muscles. *UNT* untrained subjects, *EXP* experienced rowers. P60 is in black, P90 in light gray (or green) and P120 in dark gray (or red)



For each mechanical pattern, the time lag calculated for the three comparisons (i.e., P60 vs. P90, P90 vs. P120 and P60 vs. P90) was not significantly different from zero for both populations (mean = $-0.07 \pm 0.76\%$ of the rowing cycle; range from -3 to 3%).

Individual EMG patterns

The ensemble averaged EMG patterns (\pm SD) for each muscle investigated and for each population are depicted in Fig. 3. The activity level was taken as the average of the EMG envelopes over the entire cycle. The ANOVA concerning this activity level revealed a main effect of power output for 22 of 23 muscles (p values ranged from <0.0001 to 0.004) indicating a significant increase in EMG activity with power output (Fig. 3; Tables 1, 2). In contrast, TA showed no significant change in EMG activity level with power-output ($p = 0.197$). As muscle activity was not normalized in respect with a maximal voluntary contraction (and thus no information about the degree of muscle activity was provided), the main effect of expertise could not be tested. Moreover, except for VL ($p = 0.048$) and

TraM ($p = 0.024$), no effect of expertise \times power output interaction was identified. These results indicate that EMG activity level increased globally in the same fashion for both populations, with the same muscles as major power producers.

As for the mechanical variables, the r_{\max} was calculated between power output conditions (Tables 1, 2). Overall, large similarities were found in the shape of the EMG patterns for all comparisons and for both populations (mean r_{\max} value = 0.93 ± 0.09). The ANOVA showed a main effect of expertise on the similarities for eight of the 23 muscles (i.e., GL, GM, BF, Long, Ilio, TraU, Br, and TriS). In other words, the shape of the EMG patterns was less similar between the different power outputs in UNT than EXP for GL, GM, BF, Long, Ilio and TraU. In contrast, the shapes of Br and TriS were more similar across power outputs for UNT than EXP.

The time lags for each comparison and for those of EXP and UNT are depicted in Table 3. A time lag significantly different from zero was found in 12 of the 23 muscles but remained relatively modest (maximum lag time = $-4.3 \pm 3.8\%$ of the rowing cycle for VM between P60 and

Table 1 Difference in the shape of the EMG patterns (r_{\max} values) and in muscle activity level (% increase) for the experienced rowers

experienced rowers Muscle	P60 versus P90		P60 versus P120		P90 versus P120	
	r_{\max}	Increase (%)	r_{\max}	Increase (%)	r_{\max}	Increase (%)
TA	0.94 \pm 0.05	16.9 \pm 28.1	0.92 \pm 0.04	50.4 \pm 45.9	0.93 \pm 0.08	28.5 \pm 19.9
GL	0.98 \pm 0.02	42.3 \pm 26.1	0.96 \pm 0.02	83.8 \pm 54.2	0.98 \pm 0.01	27.8 \pm 21.7
GM	0.93 \pm 0.07	28.2 \pm 29.8	0.89 \pm 0.12	70.9 \pm 54.6	0.98 \pm 0.02	31.6 \pm 23.3
Sol	0.96 \pm 0.04	9.3 \pm 22.0	0.94 \pm 0.04	27.9 \pm 50.4	0.98 \pm 0.01	14.7 \pm 36.2
VL	0.98 \pm 0.01	19.3 \pm 32.7	0.97 \pm 0.02	50.2 \pm 57.4	0.99 \pm 0.01	21.9 \pm 24.7
VM	0.98 \pm 0.02	34.1 \pm 19.5	0.97 \pm 0.02	79.5 \pm 27.7	0.99 \pm 0.01	35.1 \pm 18.3
RF	0.93 \pm 0.05	26.3 \pm 32.2	0.84 \pm 0.10	91.7 \pm 37.1	0.87 \pm 0.15	55.8 \pm 29.6
GMax	0.93 \pm 0.08	112.8 \pm 102.8	0.93 \pm 0.09	226.9 \pm 169.0	0.97 \pm 0.02	53.7 \pm 23.6
BF	0.95 \pm 0.03	37.3 \pm 25.5	0.94 \pm 0.04	78.7 \pm 11.2	0.98 \pm 0.01	33.0 \pm 19.2
ST	0.93 \pm 0.04	27.1 \pm 17.6	0.88 \pm 0.08	67.9 \pm 29.8	0.96 \pm 0.02	32.9 \pm 23.5
ES	0.90 \pm 0.14	41.2 \pm 39.0	0.90 \pm 0.13	67.5 \pm 55.2	0.91 \pm 0.20	18.9 \pm 26.7
Long	0.96 \pm 0.02	32.8 \pm 36.7	0.96 \pm 0.02	25.5 \pm 53.1	0.97 \pm 0.02	3.1 \pm 42.4
Ilio	0.97 \pm 0.02	52.5 \pm 29.5	0.97 \pm 0.02	100.7 \pm 48.6	0.98 \pm 0.01	30.7 \pm 11.0
LD	0.98 \pm 0.01	51.7 \pm 29.5	0.97 \pm 0.02	101.8 \pm 53.9	0.99 \pm 0.01	31.8 \pm 15.9
TraL	0.95 \pm 0.04	14.5 \pm 24.3	0.90 \pm 0.06	91.5 \pm 103.7	0.95 \pm 0.03	91.5 \pm 169.4
TraM	0.96 \pm 0.02	28.5 \pm 15.4	0.94 \pm 0.06	74.0 \pm 14.9	0.97 \pm 0.02	36.8 \pm 17.5
TraU	0.90 \pm 0.06	28.4 \pm 16.3	0.79 \pm 0.14	85.7 \pm 29.8	0.90 \pm 0.11	44.9 \pm 15.5
Delt	0.98 \pm 0.01	49.4 \pm 30.9	0.95 \pm 0.04	102.3 \pm 61.5	0.98 \pm 0.01	33.5 \pm 19.1
BB	0.98 \pm 0.01	25.3 \pm 18.1	0.93 \pm 0.06	75.6 \pm 44.6	0.98 \pm 0.02	40.0 \pm 28.7
Br	0.96 \pm 0.02	39.6 \pm 16.2	0.91 \pm 0.04	65.3 \pm 58.3	0.98 \pm 0.01	19.4 \pm 40.1
FD	0.96 \pm 0.02	47.56 \pm 30.0	0.93 \pm 0.04	107.1 \pm 65.9	0.97 \pm 0.02	39.1 \pm 26.9
TriL	0.95 \pm 0.04	93.5 \pm 46.7	0.92 \pm 0.05	166.5 \pm 75.9	0.98 \pm 0.01	36.6 \pm 11.9
TriS	0.94 \pm 0.03	36.2 \pm 15.3	0.90 \pm 0.05	85.3 \pm 38.6	0.98 \pm 0.02	35.2 \pm 18.3

The percentage of increase in the EMG activity level was calculated from the average of the EMG envelope over the entire cycle

Table 2 Difference in the shape of the EMG patterns (r_{\max} values) and in muscle activity level (% increase) for untrained subjects

untrained subjects Muscle	P60 versus P90		P60 versus P120		P90 versus P120	
	r_{\max}	Increase (%)	r_{\max}	Increase (%)	r_{\max}	Increase (%)
TA	0.95 ± 0.08	-3.5 ± 16.1	0.90 ± 0.05	-1.2 ± 29.7	0.95 ± 0.02	2.3 ± 24.8
GL	0.94 ± 0.05	51.7 ± 45.1	0.90 ± 0.09	98.4 ± 68.5	0.92 ± 0.14	31.1 ± 22.8
GM	0.88 ± 0.09	44.2 ± 56.9	0.85 ± 0.11	100.6 ± 113.8	0.93 ± 0.06	41.3 ± 46.4
Sol	0.93 ± 0.06	31.1 ± 29.5	0.92 ± 0.07	76.2 ± 66.3	0.98 ± 0.01	33.2 ± 29.5
VL	0.98 ± 0.01	57.4 ± 31.1	0.96 ± 0.03	97.6 ± 37.5	0.98 ± 0.02	25.9 ± 11.6
VM	0.95 ± 0.08	66.8 ± 36.7	0.94 ± 0.07	117.5 ± 49.9	0.98 ± 0.02	31.5 ± 18.9
RF	0.94 ± 0.05	36.1 ± 19.9	0.86 ± 0.10	93.5 ± 53.9	0.95 ± 0.04	42.4 ± 33.5
GMax	0.90 ± 0.08	117.2 ± 109.7	0.89 ± 0.09	320.1 ± 199.2	0.96 ± 0.03	103.1 ± 61.1
BF	0.83 ± 0.12	116.8 ± 125.3	0.77 ± 0.16	212.4 ± 169.6	0.93 ± 0.05	48.8 ± 29.4
ST	0.88 ± 0.12	78.0 ± 67.7	0.84 ± 0.10	146.9 ± 68.9	0.94 ± 0.05	43.6 ± 24.3
ES	0.94 ± 0.04	20.9 ± 39.2	0.86 ± 0.14	73.9 ± 84.6	0.92 ± 0.09	44.8 ± 61.8
Long	0.92 ± 0.05	31.7 ± 39.8	0.85 ± 0.12	57.8 ± 80.1	0.93 ± 0.04	15.7 ± 34.8
Ilio	0.91 ± 0.06	66.2 ± 72.1	0.85 ± 0.11	146.1 ± 125.7	0.93 ± 0.05	45.4 ± 27.7
LD	0.98 ± 0.02	56.8 ± 32.9	0.98 ± 0.01	132.1 ± 63.4	0.98 ± 0.01	47.1 ± 18.5
TraL	0.92 ± 0.08	44.2 ± 43.7	0.86 ± 0.15	93.2 ± 79.9	0.94 ± 0.05	33.4 ± 32.8
TraM	0.97 ± 0.02	58.7 ± 37.1	0.97 ± 0.02	108.6 ± 53.6	0.99 ± 0.01	31.6 ± 14.0
TraU	0.70 ± 0.26	41.7 ± 32.1	0.55 ± 0.22	97.4 ± 66.9	0.84 ± 0.17	41.5 ± 43.0
Delt	0.98 ± 0.01	50.8 ± 38.3	0.98 ± 0.02	115.7 ± 57.1	0.99 ± 0.01	43.1 ± 12.7
BB	0.96 ± 0.03	64.9 ± 37.1	0.94 ± 0.05	141.9 ± 91.5	0.99 ± 0.01	42.8 ± 31.9
Br	0.98 ± 0.01	66.3 ± 27.4	0.98 ± 0.01	110.3 ± 45.5	0.98 ± 0.01	25.8 ± 13.1
FD	0.96 ± 0.02	23.5 ± 64.8	0.94 ± 0.02	68.9 ± 76.8	0.97 ± 0.01	40.0 ± 21.8
TriL	0.94 ± 0.04	139.1 ± 112.0	0.95 ± 0.04	271.2 ± 190.3	0.97 ± 0.03	53.4 ± 23.3
TriS	0.97 ± 0.02	65.6 ± 37.2	0.97 ± 0.02	137.7 ± 76.3	0.99 ± 0.01	41.7 ± 17.7

The percentage of increase in the EMG activity level was calculated from the average of the EMG envelope over the entire cycle

P120). We noted that the positive time lags represented essentially the upper body muscles (Table 3). The main effect of power output was found for five of the 23 muscles (i.e., TA, TraM, BB, Br, and TriS) with p values ranging from <0.001 to 0.04 indicating that a higher lag time was found for the P60 versus P120 comparison than the others.

Muscle synergies

Using the previously described criteria, three synergies were identified at P120 for all UNT and EXP subjects, which accounted for a mean VAF of $91.1 \pm 2.4\%$ for UNT and $90.9 \pm 1.9\%$ for EXP. At P90, three synergies accounted for a mean VAF of 91.0 ± 2.0 and $89.4 \pm 1.3\%$ for UNT and EXP, respectively; and, at P60 a mean VAF of 90.1 ± 1.7 and $88.3 \pm 1.4\%$ for UNT and EXP, respectively. Thus, three muscle synergies reproduced initial EMG patterns for all subjects and all power outputs.

Figure 4 depicts the three muscle synergies (both synergy activation coefficients and muscle synergy vectors) for each power output and for UNT and EXP. Similarity in the shape

of the synergy activation coefficients between power outputs (i.e., P60 vs. P90, P90 vs. P120 and P60 vs. P120) was tested by calculating the r_{\max} . Overall, high similarities were found in these shapes across all comparisons and for the two populations (mean r_{\max} values 0.97 ± 0.03 , 0.96 ± 0.04 and 0.87 ± 0.15 for synergy #1, #2 and #3, respectively). An effect of expertise was found for synergy #2, indicating a lower similarity ($p = 0.03$) for EXP (r_{\max} across the three comparisons = 0.95 ± 0.05) compared with UNT (r_{\max} across the three comparisons = 0.97 ± 0.04). Time lags of synergy activation coefficients for each comparison and for each group (UNT and EXP) were not significantly different from zero, and neither the effect of power output nor that of expertise was found.

Concerning the muscle synergy vectors, the r values for the P60 versus P90, P60 versus P120 and P90 versus P120 comparisons were, respectively, of 0.88 ± 0.18 , 0.76 ± 0.28 and 0.90 ± 0.10 for synergy #1, 0.89 ± 0.13 , 0.73 ± 0.35 , 0.81 ± 0.40 for synergy #2, and 0.85 ± 0.19 , 0.70 ± 0.31 , 0.93 ± 0.10 for synergy #3. No effect of expertise was found.

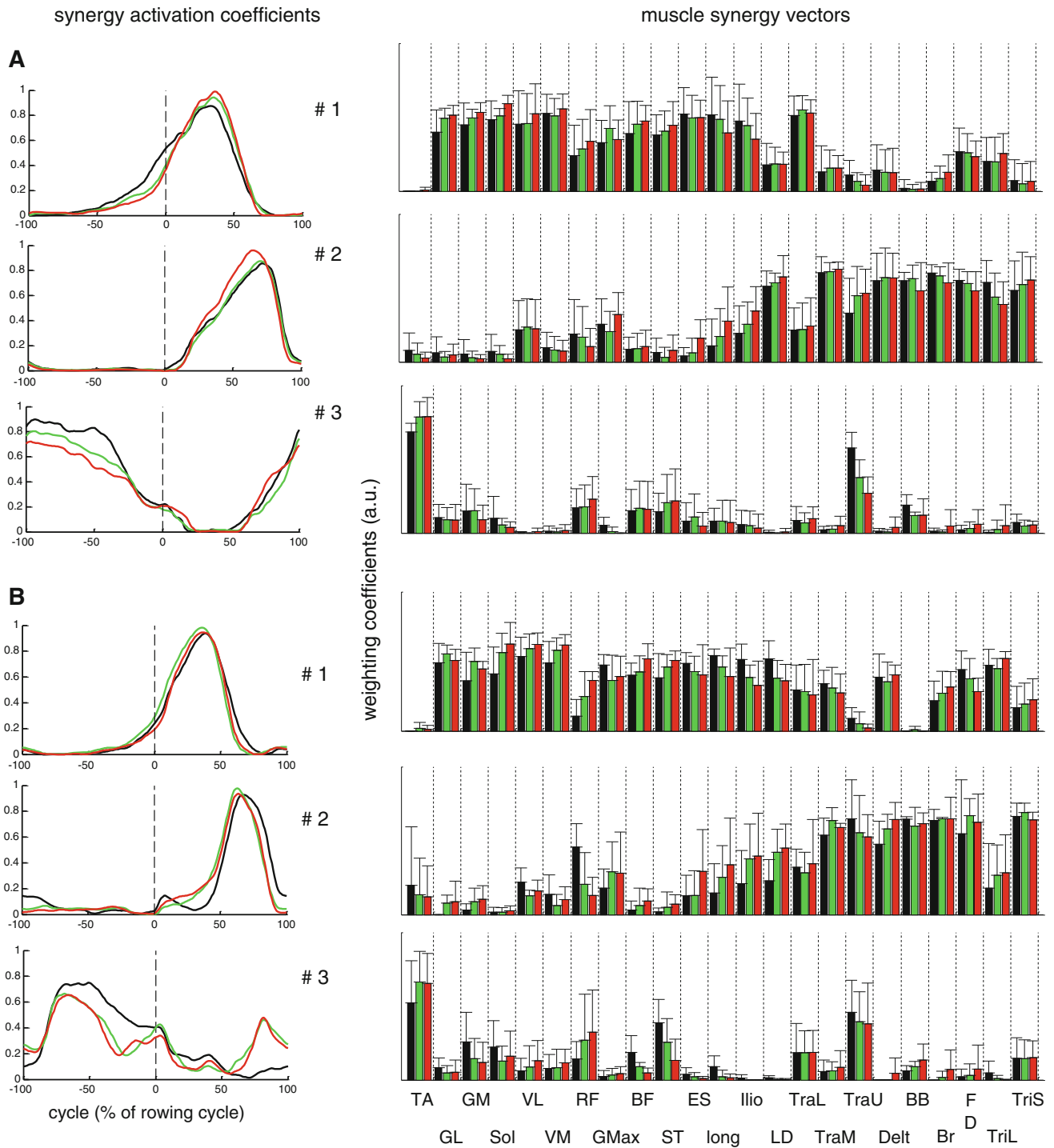


Fig. 4 Synergy activation coefficients (*left side*) and muscle synergy vectors (*right side*) depicted for the untrained subjects (**a**) and experienced (**b**) rowers. While the “muscle synergy vectors” represent the relative weighting of each muscle within each synergy, the “synergy activation coefficients” represent the relative activation of the muscle synergy across the rowing cycle. The synergy #1 engages principally the leg and trunk muscles as depicted in the weighting coefficients and is active at the very beginning of the propulsion phase (*left side* of the figure). Synergy #2 engages the

action of both the arm and trunk muscles and is active after the second part of the drive phase. Synergy #3 mainly engages TA and TraU and is associated with the recovery phase. The *vertical line* indicates the transition between the recovery and the drive phases (−100 to 0% represents the recovery phase and 0–100% represents the drive phase). *UNT* Untrained subjects, *EXP* experienced rowers. P60 is in black, P90 in light gray (or green) and P120 in dark gray (or red). See text for other abbreviations

Discussion

The aim of this study was to quantify the effect of power output on muscle coordination during rowing in both untrained subjects and experienced rowers. Despite significant changes in the level of muscle activity and in the amplitude of the mechanical variables (i.e., F_x , F_y , and F_h), the results did not show a dramatic modification in the shape of individual EMG patterns or in their timing of activation (i.e., lag time), for both UNT and EXP. The synergy analysis, which extracts the underlying structure of the activations (patterns of co-variation among multiple muscles), also showed a large consistency across the three power outputs for both populations.

Individual EMG patterns reported in the present study are in agreement with EMG patterns reported in the literature (Guével et al. 2011; Lay et al. 2002; Pollock et al. 2009; Rodriguez et al. 1990; Wilson et al. 1988). However, these previous studies recorded a limited number of

muscles (up to 12 muscles). Thus, the originality of this study is to report 23 EMG patterns and to compare them across different power outputs. In the present study, the increase in power output was partially due to an increase in stroke frequency in both populations. Changes in stroke frequency have been previously associated with kinematics and kinetic modifications (McGregor et al. 2004, 2005) and more precisely to a shift forward of the handle force as the cadence increased. Such changes were not found herein. This discrepancy could be explained by the difference in the time-scale normalization used to represent the mechanical patterns. In fact, as highlighted by Hug (2011), normalization of the rowing cycle by converting the time axis from experimentally recorded time units to an axis representing the percentage of the cycle, as done by McGregor et al. (2004, 2005), neglects changes in the duration of the different phases of the cycle as stroke frequency increased (i.e., drive and recovery phase). Therefore, that could induce artificial changes in both

Table 3 Lag time depicted for each muscle as a percentage of the rowing cycle

Muscle	P60 versus P90		P60 versus P120		P90 versus P120	
	UNT	EXP	UNT	EXP	UNT	EXP
TA	-2.1 ± 4.2	-0.7 ± 4.9	-1.3 ± 4.0	3.1 ± 3.8	0.1 ± 0.6	3.3 ± 3.5
GL	-0.9 ± 2.4	-0.4 ± 1.3	-0.5 ± 5.5	-2.4 ± 2.4	0.4 ± 2.8	-1.4 ± 1.6
GM	-2.0 ± 4.7	0.1 ± 1.8	-18.1 ± 41.1	-1 ± 1.8	0.3 ± 3.1	-1.3 ± 1.4
Sol	-2.3 ± 4.3	1.0 ± 1.5	-2.1 ± 5.5	0.4 ± 1.6	0.4 ± 1.9	-0.3 ± 0.8
VL	-1.4 ± 2.2	0.9 ± 2.5	-2.8 ± 3.4	1.0 ± 2.5	-0.6 ± 1.2	-0.3 ± 1.7
VM	-2.6 ± 2.4	0.9 ± 3.0	-4.3 ± 3.8	0.7 ± 3.0	-1.4 ± 1.8	-0.3 ± 1.8
RF	-1.0 ± 2.1	-0.6 ± 1.5	-0.8 ± 3.1	0.3 ± 1.0	0.0 ± 0.9	8.9 ± 22.6
GMax	-1.0 ± 4.0	-1.0 ± 9.5	-5.0 ± 7.9	-2.4 ± 8.0	-3.4 ± 3.8	-1.1 ± 3.1
BF	-1.0 ± 2.2	-0.6 ± 2.1	-2.9 ± 4.4	-1.3 ± 2.0	-1.1 ± 2.1	-1.0 ± 1.9
ST	-0.3 ± 3.2	0.6 ± 2.0	-1.0 ± 2.6	-1.4 ± 2.1	-0.5 ± 0.9	-1.7 ± 2.5
ES	-1.6 ± 3.8	-0.1 ± 3.3	-4.4 ± 5.6	-0.3 ± 2.2	-1.9 ± 3.2	-17.9 ± 41.6
Long	-2.8 ± 4.0	0.3 ± 1.4	-4.9 ± 10.2	-1.0 ± 1.7	-1.3 ± 3.1	-1.0 ± 1.2
Ilio	-1.9 ± 3.8	1.1 ± 2.2	-4.5 ± 9.7	-0.6 ± 2.1	-1.3 ± 2.8	-1.4 ± 1.4
LD	-0.9 ± 2.7	1.4 ± 3.4	-0.5 ± 4.1	0.9 ± 4.3	0.4 ± 1.4	-0.3 ± 1
TraL	-1.0 ± 3.2	0.7 ± 1.7	-5.5 ± 7.2	0.3 ± 1.4	-1.3 ± 2.9	-0.6 ± 0.8
TraM	0.9 ± 3.2	1.9 ± 2.0	1.1 ± 4.2	1.4 ± 2.8	0.1 ± 1.2	-0.7 ± 1
TraU	-8 ± 29.1	1.0 ± 2.3	9.1 ± 42.1	0.0 ± 2.4	1.8 ± 3.5	-1.4 ± 1.4
Delt	-0.3 ± 2.7	1.9 ± 2.5	0.0 ± 3.2	1.4 ± 1.8	-0.1 ± 0.6	-0.4 ± 1.3
BB	1.0 ± 2.8	2.3 ± 2.0	2.1 ± 4.1	2.4 ± 2.3	1.1 ± 2.3	0.1 ± 1.1
Br	0.3 ± 1.6	3.6 ± 3.2	0.3 ± 1.9	3.6 ± 3.2	0.3 ± 1.0	0.1 ± 0.9
FD	-0.8 ± 3.4	2.7 ± 2.9	-0.6 ± 4.2	2.0 ± 4.0	-0.4 ± 1.3	-1.0 ± 3.0
TriL	-1.1 ± 3.2	2.3 ± 5.3	-0.3 ± 3.3	3.1 ± 6.3	0.4 ± 0.7	0.9 ± 1.7
TriS	2.1 ± 1.7	3.1 ± 2.6	2.6 ± 2.6	2.9 ± 2.0	0.6 ± 0.9	-0.1 ± 0.9

Lags are calculated as the lag-times that maximize the cross-correlation function. A positive bias indicates that the second pattern (e.g., P90 in the P60 vs. P90 comparison) is shifted earlier in the cycle relative to the first pattern. Distributions of lags significantly different from zero ($p < 0.05$) are in bold

UNT Untrained subjects, EXP experienced rowers

mechanical and EMG patterns. To circumvent this limitation, the drive and recovery phases were time normalized separately as in previous studies (Guével et al. 2011; Janshen et al. 2009; Pollock et al. 2009).

In agreement with the mechanical patterns, muscle activity level increased with power output in 22 of the 23 muscles, whereas very few changes were found for both the shape of the EMG patterns and the timing of their activations. This is in accordance with previous results obtained during pedaling showing a consistency of muscle activity pattern while the muscle activity level varied among muscles (Wakeling et al. 2010). The absence of change in TA activity level was not surprising, as this muscle acts during the recovery phase, and that the stretcher forces did not change during this phase. It is noteworthy that GMax and TriL produced the most important increase in activity level for both populations (Fig. 3; Tables 1, 2). This result has already been reported during pedaling in GMax (Ericson 1986) and highlights the important role of these two muscles with the strategy of increasing power output during rowing. Interestingly, despite an interindividual variability (Tables 1, 2), this strategy was used in both populations and, thus, it was not linked to expertise. Nevertheless, as there is no agreement on the best normalization procedure to use (Burden and Bartlett 1999), EMG data were not normalized in the present study. Consequently, EMG activity could not be used to quantify the power output contribution of each muscle.

Five muscles (i.e., TA, TraM, BB, Br, and TriS) showed a modest but significant shift backward in their activity as power increased (Table 3), consistent with previous studies performed with different tasks such as pedaling (Hug and Dorel 2009; Wakeling and Horn 2009) or gait (Klarner et al. 2010). Recently, Guével et al. (2011) reported a similar shift backward in hamstring muscles (BF and ST) during a high intensity rowing exercise. Notably, the increase in power output in these studies and in the present work was partially due to an increase in movement velocity (i.e., cadence or stroke frequency). Assuming a constant electromechanical delay of about 100 ms (Cavanagh and Komi 1979), it would be expected that muscle activation occurs progressively earlier as movement velocity increases in order to develop force in the same part of the cycle (Li and Baum 2004). For instance, an electromechanical delay of 100 ms corresponds to 9% of the drive phase at P60 (about 27 strokes min^{-1}) and 11% of the drive phase at P120 (about 32 strokes min^{-1}). Therefore, a difference of 2% could well correspond to the lag times reported for some upper limb muscles. In contrast, the negative time lags, reported for some lower limb muscles (Table 3), cannot be accounted for by electromechanical delay considerations and would rather imply alterations in the timing of lower muscles activity.

The present results showed that three muscle synergies accounted for the majority of the variability in the surface EMG signals of 23 muscles during rowing for both UNT and EXP. To our knowledge, this is the first work to extract muscle synergies during rowing. By inspecting both synergy activation coefficients and muscle synergy vectors, it clearly appears that these three muscle synergies have a functional significance. In fact, synergy #1 engaged principally the leg and trunk muscles. It was active before the beginning of the drive, and had its peak activity before the middle of the drive phase (Fig. 4). Overall, this synergy was associated with the beginning of the propulsion phase. Interestingly, an inspection of Fig. 2 shows that this synergy had a time course roughly similar to Fx, i.e., the horizontal component of the foot-stretcher forces. This confirms previous observations highlighting the major functional role of the knee extensors to produce power on a rowing ergometer (Rodriguez et al. 1990; Wilson et al. 1988). Synergy #2 engaged the action of both the arm and trunk muscles. Its peak activity occurs after the second part of the drive phase. This second synergy was associated with the second part of the propulsion phase (Fig. 4). Synergy #3 mainly engaged TA and TraU and was associated with the recovery phase.

The consistency of muscle synergies (in terms of both synergy activation coefficients and muscle synergy vectors) across the three power outputs suggests that the motor control strategy for rowing is not altered by power output. Despite the significant time lag reported in some individual muscles (see above), synergy activation coefficients showed no time lag across power outputs. However, the inspection of Fig. 4 suggests a very slight shift of the peak of activity of the muscle synergy coefficients (that is an alteration in the shape and not in the time lag) which can be explained by the time lags found in some individual muscles.

Conclusion and practical applications

The present study showed that the motor control strategy is very little affected by power outputs on a rowing ergometer. Therefore, the fact that most of the training sessions are usually performed at a lower power output than the power output used during a 2,000-m event is not problematic from the point of view of motor control. In other words, rowers use the same temporal and spatial organization of the motor output during training and in competition. However, it should be kept in mind that muscle coordination is also linked to the muscle activity level. In this way, the high increase in GMax and TriL activity as power output increased should be considered by trainers,

e.g., specific endurance force and power training for these muscles. However, these results should be confirmed during on-water rowing. These results are also important for a better knowledge of rowing muscle activity which is an activity widely used by untrained subjects for fitness purpose.

Acknowledgments The authors are grateful to Dr. Floren COLLOUD (University of Poitiers) for the lending of the ergometer and to Dr. Arnaud Dossat, Sandra Stössel and Fabien TESSIER for their precious helps during the experiments. They also thank Dr. Thibault Deschamps for his help for the statistical analysis and Jean HUG for drawing Fig. 1. This study was supported by grants from the “Région Pays de la Loire” (Project OPERF2A). Nicolas A TURPIN was supported by a scholarship of the “Région Pays de la Loire” (Project OPERF2A).

References

- Boyas S, Nordez A, Cornu C, Guevel A (2006) Power responses of a rowing ergometer: mechanical sensors vs. Concept2 measurement system. *Int J Sports Med* 27:830–833
- Burden A, Bartlett R (1999) Normalisation of EMG amplitude: an evaluation and comparison of old and new methods. *Med Eng Phys* 21:247–257
- Cappellini G, Ivanenko YP, Poppele RE, Lacquaniti F (2006) Motor patterns in human walking and running. *J Neurophysiol* 95:3426–3437
- Cavanagh PR, Komi PV (1979) Electromechanical delay in human skeletal muscle under concentric and eccentric contractions. *Eur J Appl Physiol Occup Physiol* 42:159–163
- Colloud F, Bahuauud P, Doriot N, Champely S, Cheze L (2006) Fixed versus free-floating stretcher mechanism in rowing ergometers: mechanical aspects. *J Sports Sci* 24:479–493
- de Sèze M, Cazalets J-R (2008) Anatomical optimization of skin electrode placement to record electromyographic activity of erector spinae muscles. *Surg Radiol Anat* 30:137–143
- Ericson M (1986) On the biomechanics of cycling. A study of joint and muscle load during exercise on the bicycle ergometer. *Scand J Rehabil Med Suppl* 16:1–43
- Gordon S (2003) A mathematical model for power output in rowing on an ergometer. *Sports Eng* 6:221–234
- Guével A, Boyas S, Guihard V, Cornu C, Hug F, Nordez A (2011) Thigh muscle activities during codified training sequences of on-water rowing. *Int J Sports Med* 32(2):109–116
- Hagerman FC (1984) Applied physiology of rowing. *Sports Med* 1:303–326
- Hermens HJ, Freriks B, Disselhorst-Klug C, Rau G (2000) Development of recommendations for SEMG sensors and sensor placement procedures. *J Electromyogr Kinesiol* 10:361–374
- Hug F (2011) Can muscle coordination be precisely studied by surface electromyography? *J Electromyogr Kinesiol* 21(1):1–12
- Hug F, Dorel S (2009) Electromyographic analysis of pedaling: A review. *J Electromyogr Kinesiol* 19(2):182–198
- Hug F, Turpin NA, Guevel A, Dorel S (2010) Is interindividual variability of EMG patterns in trained cyclists related to different muscle synergies? *J Appl Physiol* 108:1727–1736
- Ivanenko YP, Poppele RE, Lacquaniti F (2004) Five basic muscle activation patterns account for muscle activity during human locomotion. *J Physiol* 556:267–282
- Ivanenko YP, Poppele RE, Lacquaniti F (2006) Motor control programs and walking. *Neuroscientist* 12:339–348
- Janshen L, Mattes K, Tidow G (2009) Muscular coordination of the lower extremities of oarsmen during ergometer rowing. *J Appl Biomech* 25:156–164
- Jorge M, Hull ML (1986) Analysis of EMG measurements during bicycle pedalling. *J Biomech* 19:683–694
- Klamer T, Chan HK, Wakeling JM, Lam T (2010) Patterns of muscle coordination vary with stride frequency during weight assisted treadmill walking. *Gait Posture* 31:360–365
- Lay BS, Sparrow WA, Hughes KM, Dwyer NJ (2002) Practice effects on coordination and control, metabolic energy expenditure, and muscle activation. *Hum Mov Sci* 21:807–830
- Lee DD, Seung HS (2001) Algorithms for non-negative matrix factorization. In: *Advances in neural information processing systems*, MIT Press, Cambridge, pp 556–562
- Li ZM (2006) Functional degree of freedom. *Mot Control* 10:301–310
- Li L, Baum BS (2004) Electromechanical delay estimated by using electromyography during cycling at different pedaling frequencies. *J Electromyogr Kinesiol* 14:647–652
- McGregor AH, Bull AM, Byng-Maddick R (2004) A comparison of rowing technique at different stroke rates: a description of sequencing, force production and kinematics. *Int J Sports Med* 25:465–470
- McGregor AH, Patankar ZS, Bull AM (2005) Spinal kinematics in elite oarswomen during a routine physiological “step test”. *Med Sci Sports Exerc* 37:1014–1020
- Muceli S, Boye AT, d’Avella A, Farina D (2010) Identifying representative synergy matrices for describing muscular activation patterns during multidirectional reaching in the horizontal plane. *J Neurophysiol* 103:1532–1542
- Pollock CL, Jenkyn TR, Jones IC, Ivanova TD, Garland SJ (2009) Electromyography and kinematics of the trunk during rowing in elite female rowers. *Med Sci Sports Exerc* 41:628–636
- Prilutsky BI (2000) Coordination of two- and one-joint muscles: functional consequences and implications for motor control. *Mot Control* 4:1–44
- Raasch CC, Zajac FE (1999) Locomotor strategy for pedaling: muscle groups and biomechanical functions. *J Neurophysiol* 82:515–525
- Rodriguez RJ, Rogriguez RP, Cook SD, Sandborn PM (1990) Electromyographic analysis of rowing stroke biomechanics. *J Sports Med Phys Fitness* 30:103–108
- Shiavi R, Frigo C, Pedotti A (1998) Electromyographic signals during gait: criteria for envelope filtering and number of strides. *Med Biol Eng Comput* 36:171–178
- Slawinski J, Dorel S, Hug F, Couturier A, Fournel V, Morin JB, Hanon C (2008) Elite long sprint running: a comparison between incline and level training sessions. *Med Sci Sports Exerc* 40:1155–1162
- Soper C, Hume PA (2004) Towards an ideal rowing technique for performance: the contributions from biomechanics. *Sports Med* 34:825–848
- Ting LH, Chvatal SA (2010) Decomposing muscle activity in motor tasks: methods and interpretation. In: Danion F, Latash M (eds) *Motor control: theories, experiments, and applications*, Oxford University Press, New York, pp 102–138
- Ting LH, McKay JL (2007) Neuromechanics of muscle synergies for posture and movement. *Curr Opin Neurobiol* 17:622–628
- Torres-Oviedo G, Macpherson JM, Ting LH (2006) Muscle synergy organization is robust across a variety of postural perturbations. *J Neurophysiol* 96:1530–1546
- Tresch MC, Saltiel P, Bizzi E (1999) The construction of movement by the spinal cord. *Nat Neurosci* 2:162–167
- Volianitis S, Secher NH (2009) Rowing, the ultimate challenge to the human body—implications for physiological variables. *Clin Physiol Funct Imaging* 29:241–244
- Wakeling JM, Horn T (2009) Neuromechanics of muscle synergies during cycling. *J Neurophysiol* 101:843

Wakeling JM, Blake OM, Chan HK (2010) Muscle coordination is key to the power output and mechanical efficiency of limb movements. *J Exp Biol* 213:487–492

Wilson MJJ, Robertson DG, Stothart JP (1988) Analysis of lower limb muscle function in ergometer rowing. *Int J Sport Biomech* 4:315–325

Zipp P (1982) Recommendations for the standardization of lead positions in surface electromyography. *Eur J Appl Physiol Occup Physiol* 50:41–54